

Article Information



Article Type:	research-article
Journal Title:	Cardiovascular Research
Publisher:	Oxford University Press
ISSN (P):	0008-6363
ISSN (E):	1755-3245
DOI Number:	10.1093/cvr/cvab367
Volume Number:	00
Issue Number:	0
First Page:	1
Last Page:	14
Copyright:	Published on behalf of the European Society of Cardiology. All rights reserved. © The Author(s) 2021. For permissions, please email: journals.permissions@oup.com.
License:	This article is published and distributed under the terms of the Oxford University Press, Standard Journals Publication Model (https://academic.oup.com/journals/pages/open_access/funder_policies/chorus/standard_publication_model)
Received Date:	27-04-2021
Editorial-decision Date:	01-12-2021
Advance Access Date:	00-00-0000
	↑

Impacts of a high-fat diet on the metabolic profile and the phenotype of atrial myocardium in mice

Left running head: N. Suffee *et al.*

Short title : Obesity and atrial cardiomyopathy

▫Nadine Suffee¹, Elodie Baptista¹, Jérôme Piquereau³, ▫Maharajah Ponnaiah³, ▫Nicolas Doisne¹, ▫Farid Ichou³, Marie Lhomme⁴, Camille Pichard¹, Vincent Galand¹, Nathalie Mougenot⁵, ▫Gilles Dilanian¹, Laurence Lucats⁶, ▫Elise Balse¹, ▫Mathias Mericksay³, ▫Wilfried Le Goff¹, and Stéphane N. Hatem^{2*} [AQ1](#) [AQ2](#)

¹INSERM UMRS1166, ICAN—Institute of Cardiometabolism and Nutrition, Sorbonne University, Paris, France;

²INSERM UMRS1166, ICAN—Institute of Cardiometabolism and Nutrition, Sorbonne University, Institute of Cardiology, Pitié-Salpêtrière Hospital, Paris, France;

³ICANalytics, Institute of Cardiometabolism and Nutrition (ICAN), Paris, France;

⁴Paris-Saclay University, Inserm UMRS 1180 Signaling and Cardiovascular Pathophysiology, Châtenay-Malabry, France;

⁵INSERM UMR_S28, Faculté de médecine Sorbonne University, Paris, France

⁶Sanofi-Aventis R&D, Cardiovascular and Metabolism Research, Chilly-Mazarin, France [AQ3](#)

The first two authors are co-first author.

Time for primary review: 37 days

Corresponding author. Tel: +33 1 40 77 95 84; fax: +33 1 40 77 96 49, E-mail: stephane.hatem@sorbonne-universite.fr [AQ4](#)

Abstract

Aims

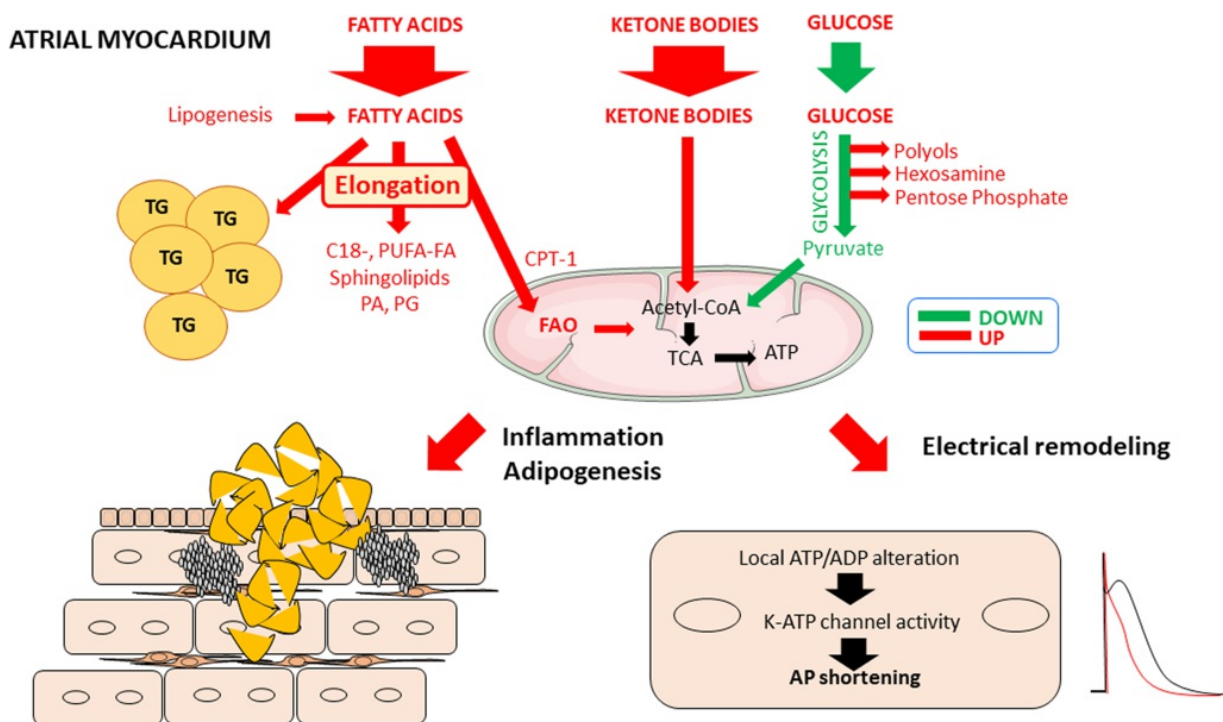
Obesity, diabetes, and metabolic syndromes are risk factors of atrial fibrillation (AF). We tested the hypothesis that metabolic disorders have a direct impact on the atria favouring the formation of the substrate of AF.

Methods and results

Untargeted metabolomic and lipidomic analysis was used to investigate the consequences of a prolonged high-fat diet (HFD) on mouse atria. Atrial properties were characterized by measuring mitochondria respiration in saponin-permeabilized trabeculae, by recording action potential (AP) with glass microelectrodes in trabeculae and ionic currents in myocytes using the perforated configuration of patch clamp technique and by several immuno-histological and biochemical approaches. After 16 weeks of HFD, obesogenic mice showed a vulnerability to AF. The atrial myocardium acquired an adipogenic and inflammatory phenotypes. Metabolomic and lipidomic analysis revealed a profound transformation of atrial energy metabolism with a predominance of long-chain lipid accumulation and beta-oxidation activation in the obese mice. Mitochondria respiration showed an increased use of palmitoyl-CoA as energy substrate. APs were short duration and sensitive to the K-ATP-dependent channel inhibitor, whereas K-ATP current was enhanced in isolated atrial myocytes of obese mouse.

Conclusion

HFD transforms energy metabolism, causes fat accumulation, and induces electrical remodelling of the atrial myocardium of mice that become vulnerable to AF.



Keywords: Atrial cardiomyopathy Atrial fibrillation Obesity Diabetes Epicardial adipose tissue Beta oxydation

[AQ5](#)

1. Introduction [AQ6](#)

Metabolic disorders, such as obesity, metabolic syndrome, or diabetes are risk factors for atrial fibrillation (AF), the most frequent cardiac arrhythmia in clinical practice.¹ For instance, each increase in body mass index is associated with 4% increase in incidence of AF. There is also a correlation between the duration of diabetes mellitus, the level of dysglycaemia and the risk of AF.²

Whether this epidemiologic association between AF and metabolic disorders is due only to shared comorbidities or also to causal pathophysiological links remains to be established. Several studies have shown that myocardial metabolism is an important determinant of the pathophysiology of AF. For instance, transcriptomics and metabolomics analysis of human atrial samples reveals the major metabolic stress of the myocardium caused by AF and characterized the predominant use of glucose and ketone bodies as the main feature. An up-regulation at both transcript³ and protein⁴ levels of several glycolytic enzymes has been observed in atrial myocardium during AF, suggesting that glycolysis overcomes the short-term energy demand. Experimental models of obesity and metabolic syndrome are characterized also by a vulnerability to AF.⁵

The epicardial adipose tissue (EAT), the abundance of which is associated with both increased incidence and prognostic of AF, could be one interface between AF and metabolic disorders.⁶⁻⁸ EAT is an important source of free fatty acid (FA) and adipokines; it regulates the redox state of the atrial myocardium.^{9,10} However, under certain clinical circumstances, EAT can secrete pro-fibrotic and pro-inflammatory factors becoming arrhythmogenic.¹¹ Furthermore, patients suffering from obesity or metabolic syndrome show more atrial EAT suggesting that metabolic disorders are an adipogenic factor for the atrial myocardium.¹²

Beneficial or detrimental effects of excess exposure of the heart to dietary FA delivery have been described depending on pre-existing cardiac diseases or the metabolic profile of the myocardium.¹³ For instance, high amount of dietary fat can cause the accumulation of lipids into the myocardium and cardiac dysfunction.¹⁴

This study examined whether an excess of dietary fat can have a direct impact on the atrial myocardium and whether it can contribute to the formation of the substrate of AF. Using unbiased lipidomic and metabolomic approaches together with physiological, histological, and biochemical analysis, we found that high FA delivery to the atria causes a shift of the oxidative profile of the atrial myocardium that become adipogenic, inflamed, and vulnerable to AF.

2. Methods

2.1 Study approval

All animal experiments were in compliance with the *Guide for the Care and Use of Laboratory Animals*, according to the Directive 2010/63/EU of the European Parliament approved by the local committee of animal care (Agreement A751320).

2.2 Experimental model and clinical study

Eight-week-old male C57Bl/6J mice (20–25 g) purchased from Janvier (CERJ, Laval, France) were subjected to 4 months of either a high-fat diet (HFD) (60% fat, D12492i Research diet) ($n = 60$) or a normal diet (ND) (8.4% fat, A04 Safe) ($n = 60$). In mice under 0.2–0.5% isoflurane anaesthesia, transthoracic echocardiography was performed and atrial burst pacing was delivered through an oesophageal probe as described in the [Supplementary material online, Methods](#).

2.3 Insulin test tolerance, glucose tolerance test

At 16 weeks diet endpoint, mice were fasted for 6 h before glucose tolerance test (GTT) or insulin test tolerance (ITT) and blood samples were collected from tail vein ([Supplementary material online, Methods](#)).

2.4 Electrophysiological measurements

APs were recorded in left atria (LA) trabeculae using glass microelectrode filled with 3-M KCl. The pharmacological study on K-ATP modulators on AP was performed by superfusing atrial trabeculae with Tyrode's solution supplemented with 30 μ M cromakalim (Sigma-Aldrich) or 1 μ M glibenclamide (Sigma-Aldrich). APs were recorded before and after drug application. Ionic currents were recorded in enzymatically isolated atrial myocytes as previously described and using the whole-cell and perforated configurations of the patch clamp technique.¹⁵

2.5 Metabolomic and lipidomic analysis

Plasma and pooled atria (right and left) were collected from mice after 4 months HFD ($n = 50$) or ND ($n = 50$), and lipidomics and metabolomics analysis were processed as described in the [Supplementary material online, Methods](#) and [Table S1](#).

2.6 Mitochondrial respiration

Mitochondrial respiration was studied *in situ* in saponin-permeabilized atrial muscle fibres using a Clarke electrode¹⁶ ([Supplementary material online, Methods](#)).

2.7 Enzyme activity

Hydroxyacyl-CoA dehydrogenase (HADHA) activity was performed at 30°C in a buffer containing 100 mM Na₂H₂P₂O₇ (pH 7.3), 1 mM EDTA (pH 7.3), 0.15 mM NADH, and 0.05 mM acetoacetyl coenzyme A with a protein concentration of 2 μ g/ μ L. Absorbance was acquired at 340 nm during 3 min

and HADHA activity was calculated using an extinction coefficient for NADH of $6220 \text{ L}\cdot\text{mol}^{-1}\cdot\text{cm}^{-1}$. Rates were given as international units (IU)/g protein.

2.8 Histology and immunofluorescence

Histology and immunofluorescence were performed with Masson's trichrome staining and immunofluorescence assays. Some sections were incubated with antibodies as described in the [Supplementary material online, Methods](#).

2.9 Flow cytometry

Cells isolated from the right and LA were washed and incubated with antibodies against CD45-APC Cy7 (clone 30-F11 eBiosciences cat# 47-0451-82), CD3-PerCp Cy5 (clone 145-2C11 eBiosciences cat #45-0031-82), CD19-PE (clone 1D3 eBiosciences cat# 12-0193-82), Ly6C-FiTC (clone AL21, eBiosciences, cat# 553104), Ly6G-PE (clone 1A8, eBiosciences, cat# 551461), and F4/80-APC (Serotec cat# MCA497APCT) as described in [Supplementary material online, Methods](#).

2.10 Transcriptomics assay

The qPCR assay was performed by using a TaqMan or Syber green gene expression assay¹⁷ ([Supplementary material online, Methods](#)).


2.11 Statistics

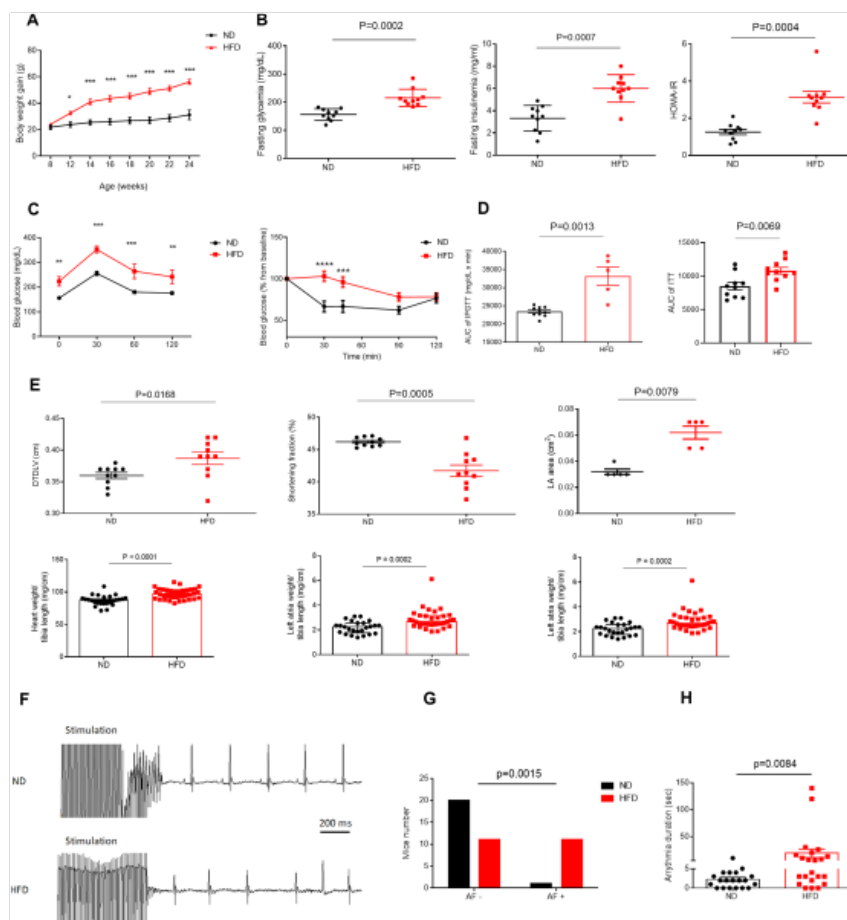
Shapiro–Wilk's normality test was performed to evaluate the normality of data distribution. Data are expressed as median with IQR using the appropriate Mann–Whitney when the data were not normally distributed. Data are expressed as means \pm SEM. Differences were investigated using the appropriate *t*-test or one-way ANOVA and a Bonferroni *post-hoc* analysis and were considered significant at $P < 0.05$. Statistical analysis was performed with GraphPad Prism 6.0 (GraphPad Software, Inc.). Statistical analyses of both the metabolomics and lipidomics data were performed using Multi Experiment Viewer statistical software package (version 4.9.0; <http://www.tm4.org/mev/>).¹⁸ Data are shown as mean \pm SEM. Comparisons of the two groups (ND and HFD) were performed by a two-tailed Student's *t*-test. Features were considered significant when the *P*-value was below 0.05 after Benjamini–Hochberg correction for false discovery rate (FDR) correction.¹⁹ The volcano plot depicting the enrichment and depletion of metabolomics and lipidomics features together with the fold change were plotted using EnhancedVolcano R package. We used Microsoft Excel to make the forest plot of individual metabolites and lipids (P -value < 0.05), the fold-change plots of the lipid species alterations (P -value < 0.05) and the mountain plots of lipid and metabolites (P -value < 0.05). The corrplot R package was used to build the correlation matrix by Pearson parametric correlations with P -value < 0.05 as significant.

3. Results

3.1 HFD induces obesity, glucose intolerance, and AF vulnerability

Mice under a prolonged, HFD gained weight and became obese at 16 weeks (46.93 ± 0.70 g and 28.74 ± 0.34 g in HFD vs. ND, respectively, $P < 0.0001$, $n = 10/\text{group}$) (*Figure 1A*). Furthermore, they displayed higher fasting glucose and insulin concentrations and exhibited altered glucose tolerance and insulin sensitivity compared to ND mice (*Figure 1B–D*).


Figure 1 HFD induces obesity, glucose intolerance, and vulnerability to atrial arrhythmia. (A) Body mass of C57BL/6J mice fed with either HFD ($n = 10$) or ND ($n = 10$) for 16 weeks. Data are expressed as mean \pm SEM; two-way ANOVA with Bonferroni's *post hoc* test. * $P = 0.0476$, *** $P = 0.0002$. (B) Blood glycaemia and insulinaemia and HOMA-IR index measured at 6 h-fasting C57BL/6J mice fed with either HFD ($n = 10$) or ND ($n = 10$) for 16 weeks. (C) Time course of blood glucose measure and (D) area under the curve of GTT and ITT obtained in HFD ($n = 5$ or 10) and ND ($n = 10$). (E) Diastolic left ventricle diameter, shortening fraction ($n = 10$), and LA surface ($n = 5$) measured using echocardiography in HFD or ND at 16 weeks. Heart and both atria (left and right) weight reported to tibia length in HFD ($n = 34$) or ND ($n = 25$) at 16 weeks. (F) Representative ECG recording of burst pacing-induced atrial arrhythmia in obese mice fed an HFD ($n = 22$) and in lean mice fed a ND ($n = 21$). (G) Histogram showing the number of mice (HFD, $n = 22$, ND, $n = 21$) from the two groups that developed AF in response to atrial burst pacing; statistical analysis was performed using a contingency χ^2 test. (H) Histogram of the arrhythmia duration (HFD, $n = 22$, ND, $n = 21$). Data are expressed as the mean \pm SEM of three independent experiments and Mann-Whitney test. 

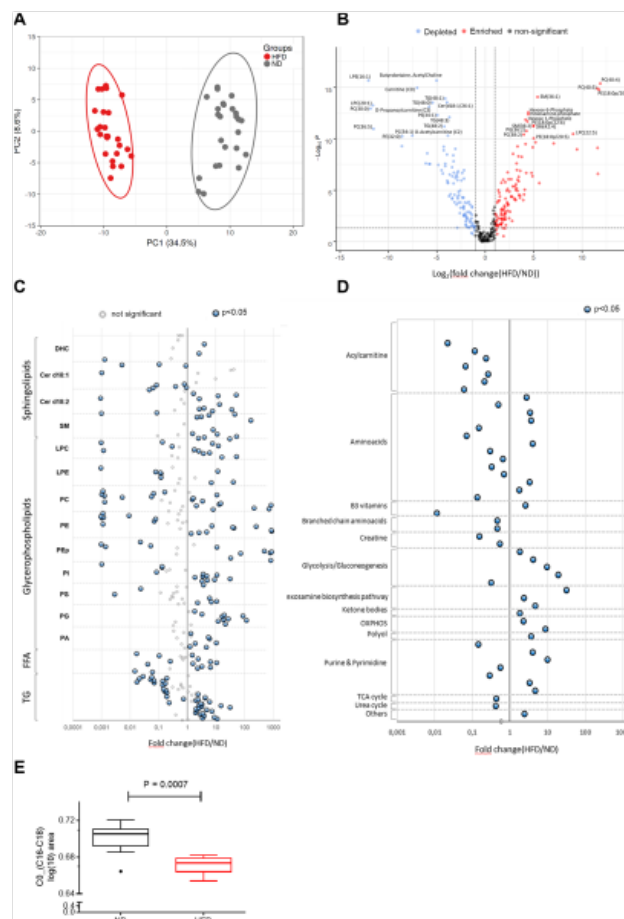


Echocardiographic examination showed a moderate dilatation of the left ventricle, together with a slight decreased systolic function and an atrial dilation in HFD mice at 16 weeks (*Figure 1E*). On electrocardiogram (ECG), P wave was slightly prolonged (16.04 ± 1.28 ms vs. 14.08 ± 1.49 ms, $P < 0.0001$), and R–R interval was shorter (104.2 ± 25.08 ms vs. 154.9 ± 24.06 ms, $P < 0.0001$) in 16-week HFD compared to ND mice. Oesophageal delivery of burst of rapid stimulation triggered an episode of AF in mice with a higher frequency and of longer duration in obese than lean animals (*Figure 1F–H*). Finally, heart and atrial weights were increased in obese mice: heart weight/tibia length (97.1 ± 1.39 mg/cm vs. 87.21 ± 1.59 mg/cm in HFD and ND mice, respectively, $P < 0.0001$); LA weight/tibia length (2.84 ± 0.13 mg/cm vs. 2.20 ± 0.10 mg/cm in HFD and ND mice, respectively, $P < 0.001$); and right atria weight/tibia length (3.72 ± 0.22 mg/cm for HFD mice vs. 2.95 ± 0.18 mg/cm $P < 0.01$) (*Figure 1E*). Taken together, these results indicate that long-lasting HFD induces a metabolic syndrome together with a moderate cardiac remodelling and vulnerability to AF in keeping with the literature.²⁰

3.2 HFD stimulates β -oxidation and lipid elongation in the atrial myocardium

The impact of HFD on lipidomic and metabolomic profile of the atrial myocardium was investigated using mass spectrometry. Principal component analysis (PCA) revealed a distinct metabolic profile between HFD and ND mice at 16 weeks (*Figure 2A*). The volcano plot showed a reduction of carnitine (C0), short-chain acylcarnitines (C2, C3), and short-chain triglycerides (TG), mostly C16, containing FAs (48:0, 48:1, and 48:3), whereas glycolysis intermediates (hexose-6-phosphate and hexose-1-phosphate), hexosamine phosphate and long-chain, mostly C18, FA phospholipids and sphingomyelins were increased upon HFD (*Figure 2B*).

Figure 2 Alteration of the metabolic profile of the atrial myocardium after prolonged HFD. (A and B) Metabolomics and lipidomics features of the atrial myocardium from HFD and ND mice after 16 weeks of diet ($n = 25$) (A) PCA score plot and (B) Volcano plot; blue, metabolites depleted; red, metabolites enriched; grey, no significant difference. $P < 0.05$, fold change ≥ 1 . (C and D) Forest plots represent individual lipids classified with respect to increasing chain length for each lipid subclass and metabolites ($n = 25$ mice in the two groups). Plots in blue represent individual (C) lipids or (D) metabolites distinct between HFD and ND conditions. (E) Histogram represents (C0)/acylcarnitine (C16) + acylcarnitine C18 ratio measured in mice atrium upon 16-week HFD compared to ND. Data are expressed as mean \pm SEM of independent experiments. Groups are compared using t -test, P -value < 0.05 corrected by FDR. 



Forest plot analysis of distribution of individual lipid species shows that 218 lipid species were significantly altered (Figure 2C) and that over 60% of them were enriched, in atria of HFD mice independently of the chain length (Figure 2C), such as sphingolipids, the negatively charged PL, PA, and PG (Supplementary material online, Figure S1A and B) [AQ7](#). For the other lipid classes, alterations were chain-length dependent with an enrichment in long and polyunsaturated and depletion in saturated and short (C16 containing lipids) species (Supplementary material online, Figure S1C–E). Overall, the atrial myocardium

of HFD mice was enriched in C18-containing lipid species as indicated by the reduction of the C16/C18 ratio in all lipid classes and by the increase in total mass of TG and FFA ([Supplementary material online, Figure S2A–C](#)).

A total of 49 metabolites were modulated by HFD (26 down-regulated and 23 up-regulated) including acylcarnitines, branched-chain amino acids, creatine while glycolysis and gluconeogenesis intermediates, hexosamine, ketone bodies, and polyols were increased (*Figure 2D*). Furthermore, transcripts for key enzymes involved in glycolysis and lipogenesis, i.e. hexokinase (HK2), acetyl-CoA carboxylase alpha (ACACA) and fatty acid synthase (FASN) were increased, whereas diacylglycerol O-acyltransferase homolog 2 was reduced ([Supplementary material online, Figure S3A](#)) in atria of 16 weeks HFD mice. The decrease in pyruvate/lactate ratio in the atrial myocardium reflecting the drop of pyruvate ([Supplementary material online, Figure S3B](#)) pointed to impairment of glycolysis.

The carnitine (C0)/acylcarnitine (C16+C18 species) ratio, which is inversely associated with the palmitoyltransferase-1 (CPT-1) activity,²¹ a key enzyme controlling the rate limiting step mitochondrial FA flux, was reduced in HFD compared to ND mice (*Figure 2E*) reflecting a higher CPT-1 activity in the former. These results indicate that in response to an excess of dietary fat the atrial myocardium accumulates long-chain FA, polyunsaturated species, and energy substrates whereas the expression of genes involved energy metabolism pathways is increased.


3.3 Distinct metabolic and lipidomic profiles between plasma and atrial myocardium

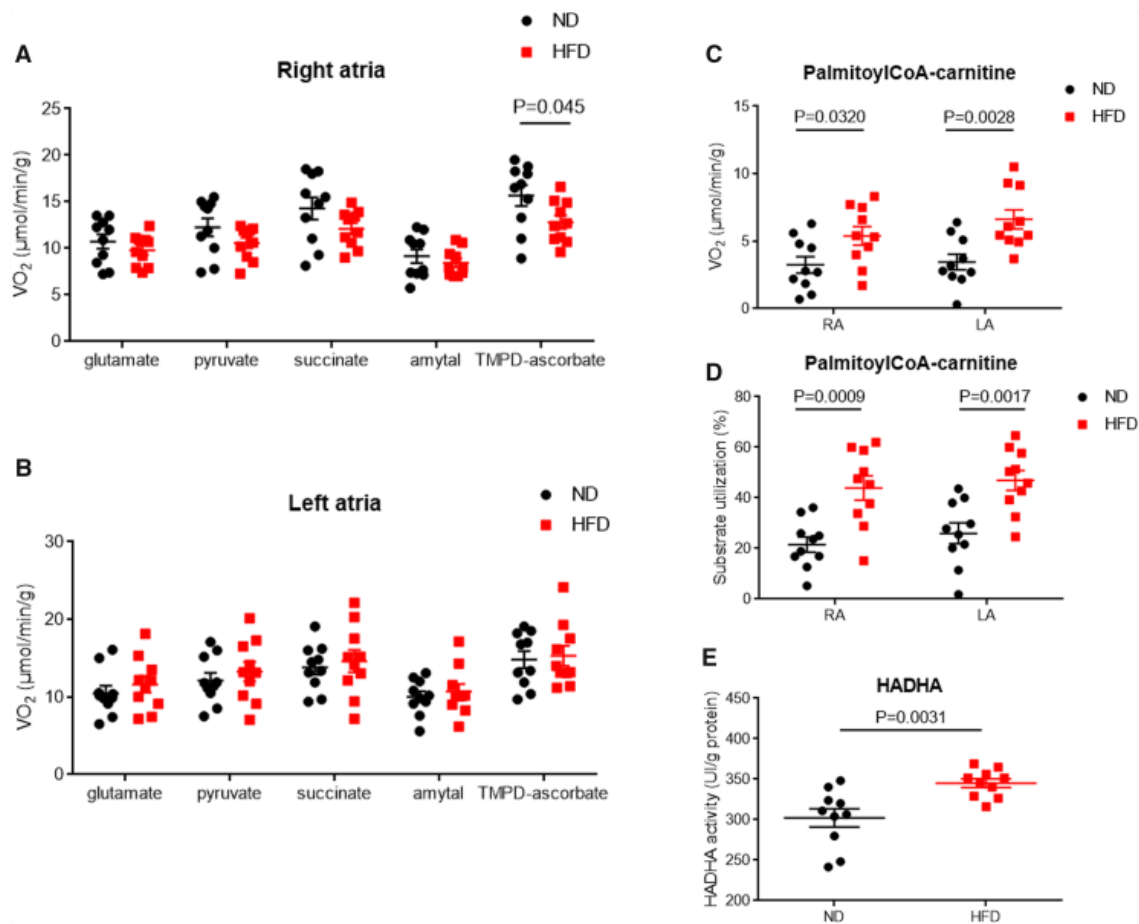
Although there was a large overlap of lipidome between atrial myocardium and plasma (*Figure 3A and B*), some alterations appeared specific to the tissue compared to plasma (*Figure 3C*), such as the increase in very long TG in the lipidome of the atrial myocardium (*Figures 2C and 3C*). The plasma from HFD mice was enriched in sphingolipids, PC and PG, carbohydrates, amino acids, ketone bodies, and polyols and depleted in PI and acylcarnitines ([Supplementary material online, Figure S4A–D](#)).

e S7B). Of note, glycolytic metabolites in the atrium were positively correlated to hexosamines and nucleotides, highlighting the use of carbons from the glucose molecule by hexosamine biosynthetic and pentose phosphate pathways at the expense of the glucose oxidation pathway.

3.4 Measurement of mitochondria respiration revealed an increased β -oxidation in atrial trabeculae from obese mice

We then examined whether this metabolic shift was associated with changes in mitochondrial respiration in HFD mice. Oxygen consumption was measured in permeabilized atrial fibres and showed that mitochondrial respiration rates were not altered after the sequential addition of glutamate (Complex I), pyruvate (production of acetyl-coA and NADH by PDH + Complex I), succinate (Complex I and II), and amytal to inhibit Complex I (Complex II) in both right and LA of HFD mice eliminating major mitochondrial dysfunction (*Figure 4A and B*). Of note, after a TMPD-ascorbate addition, a slight but significant decrease in O₂ consumption was observed only in the right atria of HFD mice (*Figure 4A and B*).

Figure 4 Measurement of mitochondria respiration revealed an increased β -oxidation in atrial trabeculae from obese mice. (A and B) Dot plots represent mitochondrial respiration rates in right (A) or left (B) atrial fibres permeable incubated with glutamate (10 mM), pyruvate (1 mM, Complex-I substrate), succinate (15 mM, Complex-II substrate), amytal (1 mM, Complex-I inhibitor), or TMPD-ascorbate (0.5 mM, Complex-IV activator) ($n = 10$). (C) The O_2 consumption was measured in both right and LA of mice upon 16-week HFD after palmitoyl-CoA-carnitne (100 μ M) addition ($n = 10$). (D) The measure of substrate utilization after PCoA-Car (100 μ M) addition was normalized with maximal O_2 consumption (V_{max}) in both left and right obesogenic mice atria compared to ND ($n = 10$). (E) The activity of HADHA was measured in mice atria upon 16-week HFD or ND ($n = 10$). Data are expressed as mean \pm SEM of independent experiments. Statistical analysis was performed using unpaired t -test. 




HFD was associated with an increase of O_2 consumption upon the addition of palmitoyl-CoA-carnitine (PCoA-Car) in both the left atrium ($6.61 \pm 0.71 \mu\text{mol } O_2/\text{min/g}$ dry weight vs. $3.45 \pm 0.58 \mu\text{mol } O_2/\text{min/g}$ dry weight in HFD and ND mice, respectively $P = 0.003$) and the right atrium ($5.39 \pm 0.69 \mu\text{mol } O_2/\text{min/g}$ dry weight vs. $3.25 \pm 0.61 \mu\text{mol } O_2/\text{min/g}$ dry weight in HFD and ND mice, respectively, $P = 0.032$)

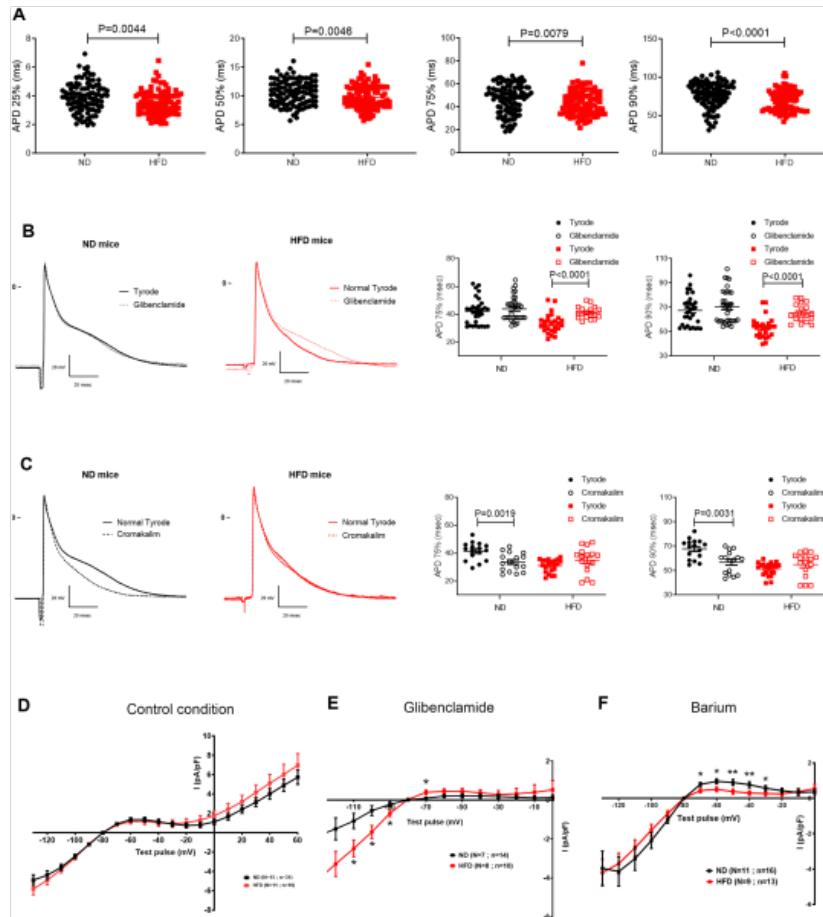
(Figure 4C). To evaluate substrate utilization, PCoA-Car was added and respiration rates were expressed as a percentage of maximal Complex I + II respiration rates. In HFD mice, a ~2-fold increase in oxygen consumption was observed in right atria ($43.94 \pm 4.78\%$ vs. $21.58 \pm 3\%$ in HFD and ND mice, respectively, $P = 0.0009$) and a 1.8-fold increase in LA ($46.9 \pm 3.96\%$ vs. $25.99 \pm 4.11\%$ in HFD and ND mice, respectively, $P = 0.0018$) (Figure 4D). These results indicate a higher capacity to use FAs by mitochondria of atrial myocardium of HFD than ND mice.

Finally, the activity of the HADHA, a key enzyme of β -oxidation, was increased in the atria of HFD mice (345.14 ± 5.40 IU/g vs. 302.35 ± 11.32 IU/g protein, HFD and ND mice, respectively, $P = 0.0031$) (Figure 4E). Taken together, these results indicate an activation of β -oxidation without major alteration of mitochondrial respiratory chain function in the atria of HFD mice.

3.5 AP shortening and K-ATP current activation in the atrial myocardium of obese mice

As myocyte excitability is tightly controlled by cellular metabolism, we next compared the electrical properties of the atria between HFD and ND mice, by recording APs in left atrial trabeculae preparation using the gold standard glass-microelectrode technique. In HFD mice, AP duration (APD) was shortened at a different time of repolarization, for instance APD₉₀ (69.46 ± 1.39 ms vs. 76.98 ± 1.65 ms in HFD and ND mice, respectively, $P < 0.0001$) (Figure 5A). A shortening of the AP was observed already after 2 weeks of HFD (Supplementary material online, Figure S8).

Figure 5 AP shortening and K-ATP current activation in the atrial myocardium of obese mice. (A) ADP measured at 25%, 50%, 75%, and 90% of the repolarization in left atrial trabeculae from HFD (red dot, $N = 97$ AP recordings, $n = 9$ mice) and ND (black dot, $N = 104$ AP recordings, $n = 11$ mice) animals. (B and C) Superimposition of AP measured at 1 Hz upon Tyrode and glibenclamide (B) or cromakalim (C) conditions and recorded after 16 weeks of diet in ND mouse atrial trabeculae; right panels, quantification of the experiments by comparing the APD 75% and APD 90% between the various conditions tested (for glibenclamide, $N = 34$ AP recordings, $n = 5$ mice; for cromakalim, $N = 16$ AP recordings, $n = 3$ mice) and HFD (for glibenclamide $N = 18$ AP recordings, $n = 5$ mice; for cromakalim experiments, $N = 16$ AP recordings, $n = 4$ mice). (D) Current–voltage relation of global potassium current measured at the end of 500 ms test pulse delivered from a holding potential of -80 mV and from -130 to $+60$ mV in perforated patch clamped atrial myocytes isolated from ND (black curve, $N = 31$ myocytes, $n = 15$ mice) and HFD (red curve, $N = 19$ myocytes, $n = 11$ mice) mice. (E) Using the same protocol as in panel D, current–voltage relation curves of subtracted component of potassium current suppressed by $5 \mu\text{M}$ glibenclamide in ND (black curve, $N = 14$ myocytes, $n = 7$ mice) and HFD (red curve, $N = 10$ myocytes, $n = 8$ mice) mice. (F) Current–voltage relation curves of subtracted component of potassium current inhibited by $500 \mu\text{M}$ barium-sensitive current in ND (black curve, $N = 16$ myocytes, $n = 11$ mice) and HFD (red curve, $N = 13$ myocytes, $n = 9$ mice) animals. Data are expressed as mean \pm SEM of independent experiments. Statistical analysis was performed using Mann–Whitney U test (A) or two-way ANOVA and Bonferroni *post hoc* test (B–F). 




K-ATP channels has been shown to constitute an important mechanistic link between metabolism and cardiac excitability,²² therefore, we decided to test the effects of K_{ATP} modulators on AP. Glibenclamide, a specific blocker of K_{ATP} channels, prolonged APD in HFD but not in ND mice, for instance at 75% (APD75: 41.28 ± 1.017 ms to 33.46 ± 1.365 ms, $P < 0.0001$) and 90% of repolarization (APD90: 53.43 ± 1.669 ms to 65.41 ± 1.772 ms, $P < 0.0001$) (Figure 5B). In contrast, cromakalim, a specific opener of ATP-sensitive potassium channels, shortened AP in ND but not in HFD mice (APD75: 41.49 ± 1.598 ms to 33.61 ± 1.653 ms, $P = 0.0034$; APD90: 67.76 ± 2.041 ms to 56.83 ± 2.253 ms, $P = 0.0031$) (Figure 5C).

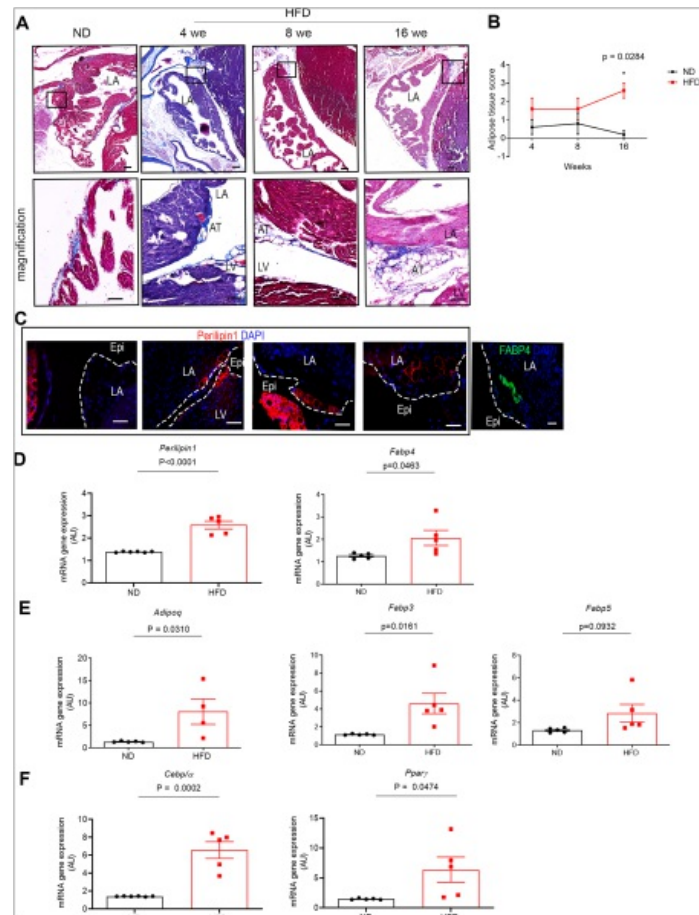
These pharmacological profiles of APs suggested an abnormal activation of K_{ATP} -dependent channels in atrial cardiomyocytes of HFD mice. However, in whole-cell configuration, no difference in potassium currents recorded between -130 and $+60$ mV was observed between HFD and ND atrial myocytes (Figure 5D). As in the whole-cell configuration, the cytosolic medium is continuously dialysed by the pipette solution, currents were recorded in the patch-perforated configuration in order to preserve the metabolic integrity of isolated atrial myocytes.²³ The various components of the inward-rectifying

potassium currents were then dissected using glibenclamide to block the I_{K-ATP} current and barium to block the I_{K1} background potassium current. As illustrated in *Figure 5E and F*, the glibenclamide-sensitive component of the inward-rectifying potassium current was enhanced, whereas the barium-sensitive component was decreased in atrial myocytes isolated from HFD mice. Finally, there was no difference of either transcript (*Kcnj11* and *Abcc8*) and protein (Kir 6.2) expression levels between HFD and ND atrial myocardium suggesting a post-transcriptional regulation of channels ([Supplementary material online, Figure S9](#)). Taken together, these results indicate that K-ATP channels are activated in atrial myocytes and could be the link between metabolic changes and AP shortening in HFD-fed mice.

3.6 An adipogenic and inflammatory responses of the atria myocardium of obese mice


In obese mouse atria some adipose tissue depots were observed in atrio-ventricle groove and also in the epicardial area¹⁷ (*Figure 6A*). The adipose tissue score, defined as the proportion of atrial surface delineated with adipocyte (alveolar shape) as previously described,²⁴ was increased in HFD mice compared to ND mice (*Figure 6B*). Furthermore, atrial myocardium of HFD mice showed an adipogenic phenotype as indicated by the increased expression at both protein and transcript levels of Perilipin-1 and FA-binding protein (Fabp)-4 (*Figure 6C and D* and [Supplementary material online, Figure S10](#)), and the increased mRNA levels for Adiponectin (*ADIPOQ*), *FABP-5*, and cardiac-specific *FABP-3* (*Figure 6E*). This adipogenic profile was observed only after 4 months of HFD. Finally, the main adipogenesis transcription factors *C/ebα* and *Pparγ* were also induced in atrial myocardium of HFD mice (*Figure 6F* and [Supplementary material online, Figure S10](#)). There was a trend towards an increased fibrosis between HFD and ND mice at 4 months.

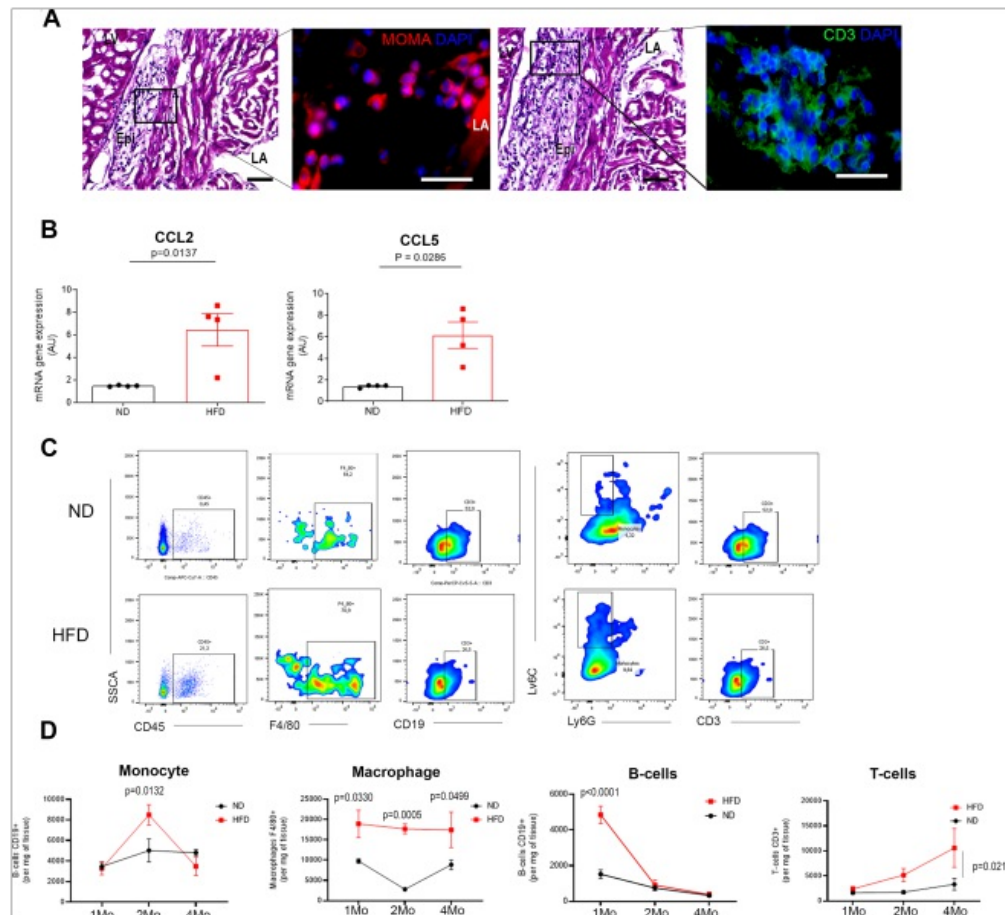
Figure 6 Activation of an adipogenic profile of the atria of MTS mice. (A) The 7 μm -thick sections of C57BL/6J mouse atrial tissue with 4 weeks (W); 8(W), or 16(W) HFD or ND stained with Masson's trichrome ($n = 5$) top and bottom squares, image magnification of the area of the epicardium layer. Scale bar, 100 and 50 μm . (B) Curves represent HFD or ND score of adipose tissue in C57BL/6J mouse atrial tissue upon 4W; 8W or 16W HFD or ND ($n = 5$). Data are expressed as mean \pm SEM of independent experiments, Two-way ANOVA, and Sidak's *post hoc*. (C) Immunofluorescence for Perilipin (red) or FABP4 (green) in C57BL/6J mouse atrial tissue with 16-W HFD ($n = 5$) or ND ($n = 5$). Scale bar 50 μm . (D–F) Transcript expression levels of adipogenic markers in C57BL/6J mouse atrial tissue upon 16-W HFD or ND ($n = 5$, each group). Data are expressed relative to the house-keeping Gapdh expression and are shown as fold change of HFD mice atria compared to ND and expressed in arbitrary units. Data are expressed as mean \pm SEM of independent experiments. Groups are compared with *t*-test in accordance with the normality test. LA, left atria; LV, left ventricle; AT, adipose tissue; Epi, epicardium. 



Inflammatory cells were detected in atrial sections of HFD and not ND mice (Figure 7A).²⁵ At the tissue level, mRNA of pro-inflammatory chemokines *CCL2* and *CCL5* were enhanced in HFD mouse atria

(Figure 7B). Moreover, mRNA expression of genes encoding for proteins of immune cells *CD45* in particular monocyte/macrophages *CD14*, *F4/80*, *CD68* and activated T cells *CD4*, *PDCD1* (Supplementa ry material online, Figure S11) were increased in the atria of HFD mice.

Figure 7 Inflammation of the atrial myocardium of obese mice. (A) Immunofluorescence staining for macrophages (MOMA) or T cells (CD3) in mice atria tissue fed a HFD ($n = 5$). (Scale bars, 100 and 50 μm). (B) Transcript expression levels of chemokines genes encoding for CCL2 or CCL5 in mice atria upon 4 months of HFD ($n = 4$ each group). Data are expressed relative to the house-keeping *Gapdh* expression and are shown as fold change of HFD mice atria compared to ND and expressed in arbitrary units. Data are expressed as mean \pm SEM of independent experiments. Groups are compared with *t*-test in accordance with the results of the normality test. (C) Dot plots represent immune cells (*CD45*), macrophages (*F4/80*), T cells (*CD3*) at 4 months, B cells (*CD19*) at 1 month, and monocyte (*Ly6Chi-Ly6Glo*) at 2 months of HFD in mice atria ($n = 5$). (D) Curves represent time course of inflammatory cells infiltration in mice atria upon 1-, 2- or 4 months of HFD compared to ND ($n = 5$). Data are expressed as mean \pm SEM two-way ANOVA with Bonferroni's *post hoc* test. LA, left atria; LV, left ventricle. 



Flow cytometry analysis of immune cells in atrial myocardium showed the presence of B cells at 1 month of HFD followed, at 2 and 4 months, by T cells. Furthermore, monocytes were detected around 2 months, whereas macrophages were detected during at all-time point of the study (*Figure 7C and D*). At the transcript level, there was no evidence for the presence of T cells *CD8*, B cells, and *CD19* in HFD atria ([Supplementary material online, Figure S11](#)). Taken together, these results indicate that the atrial myocardium of HFD mice acquired an adipogenic and inflammatory phenotype.

4. Discussion

For the first time, our study reports that during an obesogenic diet composed of a high amount of dietary fat, the atrial myocardium adopts an adaptive metabolic signature characterized by an impaired glycolysis, the predominance of FA oxidation (FAO) and it accumulates lipid. Several lines of evidences indicate that the adipogenic profile of the atrial myocardium could be the consequence of an excessive FA uptake, overwhelming FAO capacity, and resulting in atrial lipid accumulation and storage. The new metabolic and lipidomic status is associated with structural and functional remodelling of the atria that can contribute to AF vulnerability in this clinical setting.

The increase of some glycolysis intermediates likely results from the accelerated gluconeogenesis in the atrium of HFD mice rather than increased glucose uptake through insulin-sensitive atrial glucose transporters, i.e. GLUT4 and GLUT8, which are impaired during diet-induced insulin resistance.²⁶ In this vein, the content of palmitoleate (C16:1), a ‘lipokine’ intended to preserve insulin signalling,²⁷ was drastically reduced in the atrial myocardium of obese mice. Hence, the atria of dysmetabolic mice acquires a cardiac diabetic status.²⁸ The exacerbated flux of dietary lipids in HFD mice is associated with an increased oxidation of FA as indicated by the enhanced capacity of atrial mitochondria to produce energy from palmitate and by the reduction of the carnitine (C0)/acylcarnitine (C16+C18) ratio, which reflects an increased CPT-1 activity. Enhanced lipogenesis and FAO are also supported by the up-regulation of the activity of HADHA, a key enzyme of the β -oxidation pathway, and by the up regulation of *ACACA* and *FASN* genes encoding for ACACA and FA synthase, respectively. Interestingly, an enhanced FAO by the myocardium has been reported in obese patients with metabolic syndrome using PET imaging with 1-¹¹C-palmitate.²⁹ In addition to exacerbated FAO and β -oxidation other metabolites, such as ketone bodies and creatine, could constitute an important fuel for the atrium to adapt to diet-driven metabolic stress. Such metabolic plasticity of the atrial myocardium has been already reported during AF.^{4,5,29}

The enrichment in long and polyunsaturated lipids together with the increased C18 FA/C16 FA ratio in all lipid classes indicate an elongation mechanism, which could result from the induction of the expression of Elov16, an enzyme mediating the elongation of C16 FA to C18 FA, which is induced upon HFD.³⁰ Elongation of FA not only contributes to FAO but it is also a central mechanism underlying lipid storage process.³⁰ In the same line, PG species that accumulated in atrial myocardium of HFD mice has been shown to trigger lipid storage in adipose tissue.³¹ Taken together the lipidomic data and the activation of transcription factors *C/ebp α* , *Ppar γ* indicate that the atrial myocardium of obese mice stores lipids in

response to excess FA channelling. Such a storage process could result in lipid accumulation into the atrial myocardium as described at the ventricle level.¹⁴ It could also stimulate the recruitment of progenitor cells and their differentiation into adipocytes.¹⁷

Several arguments indicate that the remodelling of the electrical properties of the atria of obese mice is the consequence of the metabolic and lipidomic transformation of the atrial myocardium. First, AP shortening was observed after 2 weeks of HFD before the occurrence of the cardiac remodelling. Second, short atrial AP of obese mice shows a distinct sensitivity to K-ATP modulators. Finally, the increased glibenclamide-sensitive component of the outward potassium current in atrial myocytes of HFD mice suggests the activation of K-ATP channels. Several results indicate a post-translational regulation of K-ATP channels including the lack of difference in expression level of proteins of K-ATP channel complex. K-ATP channels are metabolic probes of the sub-sarcolemmal space. These channels are normally closed but open upon changes in the ATP/ADP ratio, during metabolism alterations or changes in lipid content. For instance, a preferential regulation of K-ATP channels by glycolysis than by the β -oxidation lipolysis has been described in both cardiomyocytes and beta islets pancreatic cells and was attributed to close physical proximity of key glycolytic enzymes to the channels into the plasma membrane.^{22,32} A shift from glycolysis to predominant FAO as in this obesity model could reduce the availability of ATP for the K-ATP channels. Another likely mechanism could be the accumulation of long-chain CoA that has been shown to prevent K-ATP channel closure and to directly activate channels.^{33,34} Whatever the exact mechanisms underlying K-ATP channel activation, these findings provide a mechanistic link between metabolism and excitability remodelling of the atria of obese mice.

Another important finding of our study is that after a prolonged obesogenic diet, the atrial myocardium becomes adipogenic. This was indicated by the accumulation of adipose tissue at epicardial surface of the atria and in the ventricle-atrial groove and by the induction of genes involved in adipogenesis encoding for PERILIPIN and ADIPONECTIN^{35,36} or transcription factors *C/EBP α* and *PPAR γ* in obese mouse atria. Transcripts of lipid protein chaperones (FABP) including the adipocyte-type *FABP4* (or *ap2*), the heart/muscle *FABP3* and the epithelial/epidermal *FABP5* were also induced in obese mouse atria.^{37–39} The FABPs facilitate the transport of FA to mitochondria⁴⁰ regulated lipid oxidation⁴¹ and storage.⁴⁰ During myocardial hypertrophy, activation of the lipogenesis and increased FA uptake are associated with an up-regulation of *Fabp4* and *Fabp5*.⁴² FABP proteins are also involved in the differentiation of adipogenic precursors derived from adipose tissue.⁴³ A correlation between *Fabp* and *Ppar γ* expression has also been reported during adipogenesis, pointing to a major adipogenic regulatory pathway.^{44–46} There are other circumstances during which atrial myocardium can acquire an adipogenic profile, such as the rapid rate of beating of sheep atria or the rapid pacing of isolated human atria.⁴⁷

Obese mice atria are characterized also by a low-grade inflammation as indicated by the presence of immune cells in the atrial myocardium composed, at the early stage of HFD, by B-cell type and, then with time, by T cells. The pro-inflammatory transcriptomic profile of the atria of obese mouse is also consistent with a low grade of inflammation of the myocardium induced by metabolic stress. In this line, it has been

reported that the adipose tissue^{11,17} or macrophages (ATM-M1)⁴⁸ can secrete pro-inflammatory chemokines during diet-induced obesity in mice. Furthermore, the chemokines CCL2 and CCL5, detected in the obese mouse atria, can favour the recruitment of CD14⁺ monocytes and their differentiation into mature macrophages expressing F4/80 and CD68. Metabolites can directly activate the immune response. For instance, dietary LC v-3 PUFA can trigger the recruitment of T cells.⁴⁹ Diet has been shown to modulate the acquisition of a pro-inflammatory phenotype by macrophages.⁵⁰

The role played by this immune response during the atrial remodelling induced by HFD remains to be established. Previous studies report that T cells are involved in the replacement of adipose tissue by fibrosis in the atria.¹¹ In the adipose tissue of obese mice, B cells favour adipocyte hypertrophy, hyperglycaemia, and the recruitment of T-cell and pro-inflammatory macrophages in obese mice.⁵¹ It remains also to determine whether macrophages detected in the atrial myocardium of obese mice derive from migration or resident subpopulation of monocytes.^{50,52}

4.1 Limitations of study

Our results have been obtained in mice that can be submitted easily to drastic changes in diet and with a cardiac energy metabolism characterized by high glycolytic component and therefore cannot be directly translate to human. However, there is evidence in humans as well of the impact of diet on energy metabolism and functional properties of the heart. For instance, in prediabetes patients, a postprandial increase in cardiac uptake of dietary FA has been directly visualized using position emission tomography imaging and has been shown to correlate with impaired pump function and reduced myocardial energy efficiency.^{28,53,54} Only male mice have been in our study. However, severe obesity can be induced by HFD in female mice together with cardiac dysfunction.⁵⁵ Finally, the exact role played by metabolic-induced atrial remodelling in the pathophysiology of AF associated with obesity cannot be firmly establishes in this study. For instance, a shortening of atrial AP has been reported in other experimental models of obesity and have been attributed to changes in L-type calcium and voltage-dependent potassium channels.^{56,57} The atrial dilation can also contribute to AF vulnerability of obese mice. Therefore, our study together with published ones indicate that the relation between obesity and AF is multifactorial and, probably, starting before the occurrence of the arrhythmia, contributing to the formation to the atrial cardiomyopathy.^{56,57}

5. Conclusion

This study indicates that HFD induces FA elongation and lipid storage together with an increase reliance on FAO of the atrial myocardium. This new metabolic phenotype is associated with a homeostasis of the atria characterized by an adipogenic and inflammatory profile and short Crefractoriness, which can contribute to the vulnerability to AF during obesity.

Supplementary material

[Supplementary material](#) is available at *Cardiovascular Research* online.

Authors' contributions

N.S., M.M., W.L.G., and S.N.H. designed research; N.S., E.Bap., G.D., J.P., N.M., V.G., C.P., F.I., M.L., M.P., and N.D. performed and analysed experiments; N.S. and J.P. contributed new reagents/analytic tools; N.S., E.Bap., J.P., G.D., M.L., F.I., M.P., E.Bal., L.L. W.L.G., M.M., N.D., and S.N.H. analysed the results and prepared the manuscript.

Conflict of interest: none declared. [AQ8](#)

Funding [AQ9](#)

This work was supported by the French National Agency through the national program *Investissements d'Avenir* (Investments for the Future), grant ANR-10-IAHU-05 (to N.S., E.Bap., G.D., F.I., M.P., M.L., E.Bal., and S.N.H.) and through the Project RHU-CARMMA, grant ANR-15-RHUS-0003 as well as the ~~Fondation de La Recherche Medicale (Foundation of Medical Research)~~ (to [Comment by Author: Fondation de France](#)) N.S., E.Bap., E.Bal., and S.N.H.). E.Bap. was funded by a PhD grant from SANOFI ('bourse CIFRE', French public/private partnership for PhD student). The project has received funding from European Union's Horizon 2020 research and innovation programme under the Grant agreement number 965286; MAESTRIA.

Data availability [AQ10](#)

The dataset has been assigned a unique digital object identifier (DOI): doi: 10.5061/dryad.z612jm6cw.

Dataset can be accessed using the unique URL: https://datadryad.org/stash/share/_Q5QGTtCRBRTtoad3aQcDhKi6ce1D8BhS-ijsNs6gbk.

Translational perspective

Understanding the link between metabolic diseases and atrial fibrillation is of major importance. One hypothesis claims that, in addition to shared comorbidities, metabolic disorders favour the substrate of atrial fibrillation. Here, we show that after prolonged high-fat diet, the atrial myocardium becomes adipogenic, inflamed, and vulnerable to atrial fibrillation. This tissue remodelling appears to result from an unbalance between uptake and oxidation of fatty acid resulting in long-chain lipid storage, activation of metabolic-sensitive potassium channels, and action potential shortening. Therefore, diet appears to be an important link between metabolic disorders and atrial fibrillation.

References

Note: this Edit/html view does not display references as per your journal style. There is no need to correct this. The content is correct and it will be converted to your journal style in the published version.

- 1 Dublin S, Glazer NL, Smith NL, Psaty BM, Lumley T, Wiggins KL, Page RL, Heckbert SR. Diabetes mellitus, glycemic control, and risk of atrial fibrillation. *J Gen Intern Med* 2010;25:853–858. [↑](#)
- 2 Bohne LJ, Johnson D, Rose RA, Wilton SB, Gillis AM. The association between diabetes mellitus and atrial fibrillation: clinical and mechanistic insights. *Front Physiol* 2019;10:135. [↑](#)
- 3 Barth AS, Merk S, Arnoldi E, Zwermann L, Kloos P, Gebauer M, Steinmeyer K, Bleich M, Käab S, Hinterseer M, Kartmann H, Kreuzer E, Dugas M, Steinbeck G, Nabauer M. Reprogramming of the human atrial transcriptome in permanent atrial fibrillation: expression of a ventricular-like genomic signature. *Circ Res* 2005;96:1022–1029. [↑](#)
- 4 Mayr M, Yusuf S, Weir G, Chung Y-L, Mayr U, Yin X, Ladroue C, Madhu B, Roberts N, De Souza A, Fredericks S, Stubbs M, Griffiths JR, Jahangiri M, Xu Q, Camm AJ. Combined metabolomic and proteomic analysis of human atrial fibrillation. *J Am Coll Cardiol* 2008;51:585–594. [↑](#)
- 5 Iwasaki Y, Shi Y, Benito B, Gillis M-A, Mizuno K, Tardif J-C, Nattel S. Determinants of atrial fibrillation in an animal model of obesity and acute obstructive sleep apnea. *Heart Rhythm* 2012;9:1409–1416.e1. [↑](#)
- 6 Al Chekatie MO, Welles CC, Metoyer R, Ibrahim A, Shapira AR, Cytron J, Santucci P, Wilber DJ, Akar JG. Pericardial fat is independently associated with human atrial fibrillation. *J Am Coll Cardiol* 2010;56:784–788. [↑](#)
- 7 Thanassoulis G, Massaro JM, O'Donnell CJ, Hoffmann U, Levy D, Ellinor PT, Wang TJ, Schnabel RB, Vasan RS, Fox CS, Benjamin EJ. Pericardial fat is associated with prevalent atrial fibrillation: the Framingham Heart Study. *Circ Arrhythm Electrophysiol* 2010;3:345–350. [↑](#)
- 8 Wong CX, Abed HS, Molaei P, Nelson AJ, Brooks AG, Sharma G, Leong DP, Lau DH, Middeldorp ME, Roberts-Thomson KC, Wittert GA, Abhayaratna WP, Worthley SG, Sanders P. Pericardial fat is associated with atrial fibrillation severity and ablation outcome. *J Am Coll Cardiol* 2011;57:1745–1751. [↑](#)
- 9 Antonopoulos AS, Margaritis M, Verheule S, Recalde A, Sanna F, Herdman L, Psarros C, Nasrallah H, Coutinho P, Akoumianakis I, Brewer AC, Sayeed R, Krasopoulos G, Petrou M, Tarun A, Tousoulis D, Shah AM, Casadei B, Channon KM, Antoniades C. Mutual regulation of epicardial adipose tissue and myocardial redox state by PPAR- γ /adiponectin signalling. *Circ Res* 2016;118:842–855. [↑](#)

- 10 Villasante Fricke AC, Iacobellis G. Epicardial adipose tissue: clinical biomarker of cardio-metabolic risk. *Int J Mol Sci* 2019;20:5989. [↑](#)
- 11 Haemers P, Hamdi H, Guedj K, Suffee N, Farahmand P, Popovic N, Claus P, LePrince P, Nicoletti A, Jalife J, Wolke C, Lendeckel U, Jaïs P, Willems R, Hatem SN. Atrial fibrillation is associated with the fibrotic remodelling of adipose tissue in the subepicardium of human and sheep atria. *Eur Heart J* 2017;38:53–61. [↑](#)
- 12 Mahajan R, Nelson A, Pathak RK, Middeldorp ME, Wong CX, Twomey DJ, Carbone A, Teo K, Agbaedeng T, Linz D, Groot J. D, Kalman JM, Lau DH, Sanders P. Electroanatomical remodeling of the atria in obesity: impact of adjacent epicardial fat. *JACC Clin Electrophysiol* 2018;4:1529–1540. [↑](#)
- 13 Carpentier AC. Abnormal myocardial dietary fatty acid metabolism and diabetic cardiomyopathy. *Can J Cardiol* 2018;34:605–614. [↑](#)
- 14 Goldberg IJ, Trent CM, Schulze PC. Lipid metabolism and toxicity in the heart. *Cell Metab* 2012;15:805–812. [↑](#)
- 15 Boycott HE, Barbier CSM, Eichel CA, Costa KD, Martins RP, Louault F, Dilanian G, Coulombe A, Hatem SN, Balse E. Shear stress triggers insertion of voltage-gated potassium channels from intracellular compartments in atrial myocytes. *Proc Natl Acad Sci USA* 2013;110:E3955–E3964. [↑](#)
- 16 Sanz M-N, Grimbert L, Moulin M, Gressette M, Rucker-Martin C, Lemaire C, Mericskay M, Veksler V, Ventura-Clapier R, Garnier A, Piquereau J. Inducible cardiac-specific deletion of Sirt1 in male mice reveals progressive cardiac dysfunction and sensitization of the heart to pressure overload. *Int J Mol Sci* 2019;20:5005. [↑](#)
- 17 Suffee N, Moore-Morris T, Farahmand P, Rucker-Martin C, Dilanian G, Fradet M, Sawaki D, Derumeaux G, LePrince P, Clément K, Dugaïl I, Puceat M, Hatem SN. Atrial natriuretic peptide regulates adipose tissue accumulation in adult atria. *Proc Natl Acad Sci USA* 2017;114:E771–E780. [↑](#)
- 18 Saeed AI, Sharov V, White J, Li J, Liang W, Bhagabati N, Braisted J, Klapa M, Currier T, Thiagarajan M, Sturn A, Snuffin M, Rezantsev A, Popov D, Ryltsov A, Kostukovich E, Borisovsky I, Liu Z, Vinsavich A, Trush V, Quackenbush J. TM4: a free, open-source system for microarray data management and analysis. *BioTechniques* 2003;34:374–378. [↑](#)
- 19 Klipper-Aurbach Y, Wasserman M, Braunspiegel-Weintrob N, Borstein D, Peleg S, Assa S, Karp M, Benjamini Y, Hochberg Y, Laron Z. Mathematical formulae for the prediction of the residual beta cell function during the first two years of disease in children and adolescents with insulin-dependent diabetes mellitus. *Med Hypotheses* 1995;45:486–490. [↑](#)
- 20 Costantino S, Akhmedov A, Melina G, Mohammed SA, Othman A, Ambrosini S, Wijnen WJ, Sada L, Ciavarella GM, Liberale L, Tanner FC, Matter CM, Hornemann T, Volpe M, Mechta-Grigoriou F,

- Camici GG, Sinatra R, Lüscher TF, Paneni F. Obesity-induced activation of JunD promotes myocardial lipid accumulation and metabolic cardiomyopathy. *Eur Heart J* 2019;40:997–1008. [↑](#)
- 21 Knottnerus SJG, Bleeker JC, Wüst RCI, Ferdinandusse S, IJlst L, Wijburg FA, Wanders RJA, Visser G, Houtkooper RH. Disorders of mitochondrial long-chain fatty acid oxidation and the carnitine shuttle. *Rev Endocr Metab Disord* 2018;19:93–106. [↑](#)
- 22 Csonka C, Kupai K, Bencsik P, Görbe A, Pálóczi J, Zvara A, Puskás LG, Csont T, Ferdinandy P. Cholesterol-enriched diet inhibits cardioprotection by ATP-sensitive K⁺ channel activators cromakalim and diazoxide. *Am J Physiol Heart Circ Physiol* 2014;306:H405–H413. [↑](#)
- 23 Akaike N, Harata N. Nystatin perforated patch recording and its applications to analyses of intracellular mechanisms. *Jpn J Physiol* 1994;44:433–473. [↑](#)
- 24 Marcelin G, Da Cunha C, Gamblin C, Suffee N, Rouault C, Leclerc A, Lacombe A, Sokolovska N, Gautier EL, Clément K, Dugail I. Autophagy inhibition blunts PDGFRA adipose progenitors' cell-autonomous fibrogenic response to high-fat diet. *Autophagy* 2020;16:2156–2111. [↑](#)
- 25 Furuhashi M, Fucho R, Görgün CZ, Tuncman G, Cao H, Hotamisligil GS. Adipocyte/macrophage fatty acid-binding proteins contribute to metabolic deterioration through actions in both macrophages and adipocytes in mice. *J Clin Invest* 2008;118:2640–2650. [↑](#)
- 26 Maria Z, Campolo AR, Scherlag BJ, Ritchey JW, Lacombe VA. Dysregulation of insulin-sensitive glucose transporters during insulin resistance-induced atrial fibrillation. *Biochim Biophys Acta Mol Basis Dis* 2018;1864:987–996. [↑](#)
- 27 Cao H, Gerhold K, Mayers JR, Wiest MM, Watkins SM, Hotamisligil GS. Identification of a lipokine, a lipid hormone linking adipose tissue to systemic metabolism. *Cell* 2008;134:933–944. [↑](#)
- 28 Noll C, Kunach M, Frisch F, Bouffard L, Dubreuil S, Jean-Denis F, Phoenix S, Cunnane SC, Guérin B, Turcotte EE, Carpentier AC. Seven-day caloric and saturated fat restriction increases myocardial dietary fatty acid partitioning in impaired glucose-tolerant subjects. *Diabetes* 2015;64:3690–3699. [↑](#)
- 29 Ussher JR, Elmariah S, Gerszten RE, Dyck JRB. The emerging role of metabolomics in the diagnosis and prognosis of cardiovascular disease. *J Am Coll Cardiol* 2016;68:2850–2870. [↑](#)
- 30 Matsuzaka T, Shimano H. Elovl6: a new player in fatty acid metabolism and insulin sensitivity. *J Mol Med Berl Ger* 2009;87:379–384. [↑](#)
- 31 Kayser BD, Lhomme M, Prifti E, Da Cunha C, Marquet F, Chain F, Naas I, Pelloux V, Dao M-C, Kontush A, Rizkalla SW, Aron-Wisnewsky J, Bermúdez-Humarán LG, Oakley F, Langella P, Clément K, Dugail I. Phosphatidylglycerols are induced by gut dysbiosis and inflammation, and favorably modulate adipose tissue remodeling in obesity. *FASEB J* 2019;33:4741–4754. [↑](#)

- 32 Weiss JN, Lamp ST. Cardiac ATP-sensitive K⁺ channels. Evidence for preferential regulation by glycolysis. *J Gen Physiol* 1989;94:911–935. [↑](#)
- 33 Liu GX, Hanley PJ, Ray J, Daut J. Long-chain acyl-coenzyme A esters and fatty acids directly link metabolism to K(ATP) channels in the heart. *Circ Res* 2001;88:918–924. [↑](#)
- 34 Schulze D, Rapedius M, Krauter T, Baukrowitz T. Long-chain acyl-CoA esters and phosphatidylinositol phosphates modulate ATP inhibition of KATP channels by the same mechanism. *J Physiol* 2003;552:357–367. [↑](#)
- 35 Liao Y, Takashima S, Maeda N, Ouchi N, Komamura K, Shimomura I, Hori M, Matsuzawa Y, Funahashi T, Kitakaze M. Exacerbation of heart failure in adiponectin-deficient mice due to impaired regulation of AMPK and glucose metabolism. *Cardiovasc Res* 2005;67:705–713. [↑](#)
- 36 Ouchi N, Parker JL, Lugus JJ, Walsh K. Adipokines in inflammation and metabolic disease. *Nat Rev Immunol* 2011;11:85–97. [↑](#)
- 37 Lopez-Canoa JN, Baluja A, Couselo-Seijas M, Naveira AB, Gonzalez-Melchor L, Rozados A, Martínez-Sande L, García-Seara J, Fernandez-Lopez XA, Fernandez AL, Gonzalez-Juanatey JR, Eiras S, Rodriguez-Mañero M. Plasma FABP4 levels are associated with left atrial fat volume in persistent atrial fibrillation and predict recurrence after catheter ablation. *Int J Cardiol* 2019;292:131–135. [↑](#)
- 38 Shingu Y, Yokota T, Takada S, Niwano H, Ooka T, Katoh H, Tachibana T, Kubota S, Matsui Y. Decreased gene expression of fatty acid binding protein 3 in the atrium of patients with new onset of atrial fibrillation in cardiac perioperative phase. *J Cardiol* 2018;71:65–70. [↑](#)
- 39 Umbarawan Y, Syamsunarno MRAA, Obinata H, Yamaguchi A, Sunaga H, Matsui H, Hishiki T, Matsuura T, Koitabashi N, Obokata M, Hanaoka H, Haque A, Kunimoto F, Tsushima Y, Suematsu M, Kurabayashi M, Iso T. Robust suppression of cardiac energy catabolism with marked accumulation of energy substrates during lipopolysaccharide-induced cardiac dysfunction in mice. *Metabolism* 2017;77:47–57. [↑](#)
- 40 Rodríguez-Calvo R, Girona J, Rodríguez M, Samino S, Barroso E, de Gonzalo-Calvo D, Guaita-Esteruelas S, Heras M, van der Meer RW, Lamb HJ, Yanes O, Correig X, Llorente-Cortés V, Vázquez-Carrera M, Masana L. Fatty acid binding protein 4 (FABP4) as a potential biomarker reflecting myocardial lipid storage in type 2 diabetes. *Metabolism* 2019;96:12–21. [↑](#)
- 41 Bonen A, Holloway GP, Tandon NN, Han X-X, McFarlan J, Glatz JFC, Luiken JJFP. Cardiac and skeletal muscle fatty acid transport and transporters and triacylglycerol and fatty acid oxidation in lean and Zucker diabetic fatty rats. *Am J Physiol Regul Integr Comp Physiol* 2009;297:R1202–R1212. [↑](#)
- 42 Umbarawan Y, Syamsunarno MRAA, Koitabashi N, Yamaguchi A, Hanaoka H, Hishiki T, Nagahata-Naito Y, Obinata H, Sano M, Sunaga H, Matsui H, Tsushima Y, Suematsu M, Kurabayashi M, Iso T.

Glucose is preferentially utilized for biomass synthesis in pressure-overloaded hearts: evidence from fatty acid-binding protein-4 and -5 knockout mice. *Cardiovasc Res* 2018;114:1132–1144. ↑

43 Samulin J, Berget I, Lien S, Sundvold H. Differential gene expression of fatty acid binding proteins during porcine adipogenesis. *Comp Biochem Physiol B Biochem Mol Biol* 2008;151:147–152. ↑

44 Fajas L, Landsberg RL, Huss-Garcia Y, Sardet C, Lees JA, Auwerx J. E2Fs regulate adipocyte differentiation. *Dev Cell* 2002;3:39–49. ↑

45 Ren D, Collingwood TN, Rebar EJ, Wolffe AP, Camp HS. PPARgamma knockdown by engineered transcription factors: exogenous PPARgamma2 but not PPARgamma1 reactivates adipogenesis. *Genes Dev* 2002;16:27–32. ↑

46 Saladin R, Fajas L, Dana S, Halvorsen YD, Auwerx J, Briggs M. Differential regulation of peroxisome proliferator activated receptor gamma1 (PPARgamma1) and PPARgamma2 messenger RNA expression in the early stages of adipogenesis. *Cell Growth Differ Mol Biol J Am Assoc Cancer Res* 1999;10:43–48. ↑

47 Chilukoti RK, Giese A, Malenke W, Homuth G, Bukowska A, Goette A, Felix SB, Kanaan J, Wollert H-G, Evert K, Verheule S, Jais P, Hatem SN, Lendeckel U, Wolke C. Atrial fibrillation and rapid acute pacing regulate adipocyte/adipositas-related gene expression in the atria. *Int J Cardiol* 2015;187:604–613. ↑

48 Mantovani A, Sica A, Sozzani S, Allavena P, Vecchi A, Locati M. The chemokine system in diverse forms of macrophage activation and polarization. *Trends Immunol* 2004;25:677–686. ↑

49 Liddle DM, Hutchinson AL, Monk JM, Power KA, Robinson LE. Dietary ω-3 polyunsaturated fatty acids modulate CD4+ T-cell subset markers, adipocyte antigen-presentation potential, and NLRP3 inflammasome activity in a coculture model of obese adipose tissue. *Nutrition* 2021;91–92:111388. ↑

50 Félix I, Jokela H, Karhula J, Kotaja N, Savontaus E, Salmi M, Rantakari P. Single-cell proteomics reveals the defined heterogeneity of resident macrophages in white adipose tissue. *Front Immunol* 2021;12:719979. ↑

51 Frasca D, Blomberg BB. Obesity accelerates age defects in mouse and human B cells. *Front Immunol* 2020;11:2060. ↑

52 Wong NR, Mohan J, Kopecky BJ, Guo S, Du L, Leid J, Feng G, Lokshina I, Dmytrenko O, Luehmann H, Bajpai G, Ewald L, Bell L, Patel N, Bredemeyer A, Weinheimer CJ, Nigro JM, Kovacs A, Morimoto S, Bayguinov PO, Fisher MR, Stump WT, Greenberg M, Fitzpatrick JAJ, Epelman S, Kreisel D, Sah R, Liu Y, Hu H, Lavine KJ. Resident cardiac macrophages mediate adaptive myocardial remodeling. *Immunity* 2021;54:2072–2088.e7. ↑

53 Labbé SM, Grenier-Larouche T, Croteau E, Normand-Lauzière F, Frisch F, Ouellet R, Guérin B, Turcotte EE, Carpentier AC. Organ-specific dietary fatty acid uptake in humans using positron emission

tomography coupled to computed tomography. *Am J Physiol Endocrinol Metab* 2011;300:E445–E453. [↑](#)

54 Labbé SM, Grenier-Larouche T, Noll C, Phoenix S, Guérin B, Turcotte EE, Carpentier AC. Increased myocardial uptake of dietary fatty acids linked to cardiac dysfunction in glucose-intolerant humans. *Diabetes* 2012;61:2701–2710. [↑](#)


55 John C, Grune J, Ott C, Nowotny K, Deubel S, Kühne A, Schubert C, Kintscher U, Regitz-Zagrosek V, Grune T. Sex differences in cardiac mitochondria in the New Zealand obese mouse. *Front Endocrinol* 2018;9:732. [↑](#)


56 Aromolaran AS, Colecraft HM, Boutjdir M. High-fat diet-dependent modulation of the delayed rectifier K(+) current in adult guinea pig atrial myocytes. *Biochem Biophys Res Commun* 2016;474:554–559. [↑](#)


57 Martinez-Mateu L, Saiz J, Aromolaran AS. Differential modulation of IK and ICa,L channels in high-fat diet-induced obese guinea pig atria. *Front Physiol* 2019;10:1212. [↑](#)


Author Query


- Query:** [AQ1] - : Please check all author names and affiliations. Please check that author surnames have been identified by a pink background in the PDF version, and by green text in the html proofing tool version (if applicable). This is to ensure that forenames and surnames have been correctly tagged for online indexing.


Response: [Author - hatem: stephane.hatem@upmc.fr]: Accept 
- Query:** [AQ2] - : Please indicate the missing affiliation designator '5' in the author line and also provide the missing affiliation '3' in the affiliation line.


Response: [Author - hatem: stephane.hatem@upmc.fr]: -Nathalie Mougenot affiliation 5 is OK- Mathias Meriskay is affiliation 4 and not 3 
- Query:** [AQ3] - : Please provide the department details for all affiliations.

Response: [Author - hatem: stephane.hatem@upmc.fr]: Accept 
- Query:** [AQ4] - : Please check whether the tel, fax numbers and email address of the corresponding author are OK as set.

Response: [Author - hatem: stephane.hatem@upmc.fr]: Accept 
- Query:** [AQ5] - : If your manuscript has figures or text from other sources, please ensure you have permission from the copyright holder. For any questions about permissions contact jnls.author.support@oup.com.

Response: [Author - hatem: stephane.hatem@upmc.fr]: Accept 
- Query:** [AQ6] - : Please check whether the section hierarchy is OK as set.

Response: [Author - hatem: stephane.hatem@upmc.fr]: Accept 
- Query:** [AQ7] - : Please provide the expansion of PL, PA, PG, SFA, MUFA, AA and TMPD in the first occurrence.


Response: [Author - hatem: stephane.hatem@upmc.fr]: PL, PhospholipidPA,phosphatidicacid;PG,phosphatidylglycerolSFA, saturated fatty acidMUFA, monounsaturated fatty acidAA, arachidonic acidTMPD, tetamethylenediamine 
- Query:** [AQ8] - : You may need to include a 'conflict of interest' section. This would cover any situations that might raise any questions of bias in your work and in your article's conclusions, implications, or opinions. Please see https://academic.oup.com/journals/pages/authors/authors_faqs/conflicts_of_interest.

Response: [Author - *hatem: stephane.hatem@upmc.fr*]: Accept 

9. **Query:** [AQ9] - : Please check that funding is recorded in a separate funding section if applicable. Use the full official names of any funding bodies, and include any grant numbers. Please ensure that this detail has been provided in the author comments before accepting this query.

Response: [Author - *hatem: stephane.hatem@upmc.fr*]: Fondation de la recherche Meciale must be replaced by **Fondation de France** 

10. **Query:** [AQ10] - : Journal policy requires authors to provide a data availability statement in their manuscript. Please confirm that this statement is included in your manuscript and that any required links or identifiers for your data are present in the manuscript as described or provide edits with the required information. Please see the sample data availability statements at https://academic.oup.com/journals/pages/authors/preparing_your_manuscript/research-data-policy#data2.

Response: [Author - *hatem: stephane.hatem@upmc.fr*]: Accept 

Comments

1. **Comments** [Author - 12/24/2021 1:07:05 PM]: Fondation de France 